

Linking Development and Determinacy with Organic Acid Efflux from Proteoid Roots of White Lupin Grown with Low Phosphorus and Ambient or Elevated Atmospheric CO₂ Concentration¹

Michelle Watt and John R. Evans*

Environmental Biology Group, Research School of Biological Sciences, Australian National University, P.O. Box 475, Canberra, ACT, Australia 2601

White lupin (*Lupinus albus* L.) was grown in hydroponic culture with 1 μM phosphorus to enable the development of proteoid roots to be observed in conjunction with organic acid exudation. Discrete regions of closely spaced, determinate secondary laterals (proteoid rootlets) emerged in near synchrony on the same plant. One day after reaching their final length (4 mm), citrate exudation occurred over a 3-d pulse. The rate of exudation varied diurnally, with maximal rates during the photoperiod. At the onset of citrate efflux, rootlets had exhausted their apical meristems and had differentiated root hairs and vascular tissues along their lengths. Neither *in vitro* phosphoenolpyruvate carboxylase nor citrate synthase activity was correlated with the rate of citrate exudation. We suggest that an unidentified transport process, presumably at the plasma membrane, regulates citrate efflux. Growth with elevated (700 $\mu\text{L L}^{-1}$) atmospheric [CO₂] promoted earlier onset of rootlet determinacy by 1 d, resulting in shorter rootlets and citrate export beginning 1 d earlier as a 2-d diurnal pulse. Citrate was the dominant organic acid exported, and neither the rate of exudation per unit length of root nor the composition of exudate was altered by atmospheric [CO₂].

Proteoid roots develop on a range of plant species, including white lupin (*Lupinus albus* L.), adapted to environments with poorly available phosphorus (Gardner et al., 1981; Dinkelaker et al., 1995). First described in 1960 in a study of the Proteaceae (Purnell, 1960), proteoid roots have discrete clusters of closely spaced laterals (rootlets) along their lengths that greatly increase the surface area for nutrient uptake compared with the proteoid root axis (Lamont et al., 1984). These clusters of rootlets release exudates, notably organic acids that can solubilize phosphorus by chelating the metal ions that immobilize it (Gardner et al., 1983; Gerke et al., 1994). The organic acids exported from white lupin proteoid roots can include citrate, malate, succinate, and fumarate (Gardner et al., 1983; Dinkelaker et al., 1989; Johnson et al., 1994; Keerthisinghe et al., 1998) and can account for a substantial portion of the total plant carbon. For example, Dinkelaker et al. (1989) showed that citrate exported from white lupin growing in a calcareous

soil was 23% of the plant dry weight at 13 weeks, and Johnson et al. (1996b) measured malate, succinate, and citrate totaling 12% of the plant dry weight at 3 weeks.

The metabolism linked to the synthesis and efflux of organic acids from proteoid roots has been studied recently in white lupin (Johnson et al., 1994, 1996a, 1996b). Johnson et al. (1996a) showed that approximately 30% of the carbons released from the roots as malate or citrate were fixed within the proteoid roots by the enzyme PEPC (EC 4.1.1.31). The increased activity and expression of PEPC and malate dehydrogenase (EC 1.1.1.37) coincided with the start of organic acid efflux and was considered to be part of an altered metabolism within proteoid roots that was required for the synthesis of the exported organic acids (Johnson et al., 1996b).

The morphology and anatomy of proteoid rootlets was reported previously for some members of the Proteaceae (for summary, see Dinkelaker et al., 1995; Skene et al., 1996, 1998a, 1998b). These studies showed that a cluster of rootlets starts as many meristematic primordia that subsequently mature into determinate rootlets with no apical meristem and root hairs around their tips. In *Hakea obliqua*, approximately 5 d is required for the rootlets to reach their final determinate length (Dell et al., 1980). To our knowledge, there are no published studies of the anatomy of white lupin proteoid rootlets, although macrographs of white lupin rootlets growing in calcareous soil show root hairs extending around their tips (Dinkelaker et al., 1989), suggesting that the rootlets also reach a determinate stage.

There is evidence that the efflux of exudates, including organic acids, occurs when rootlets are young and that this efflux is transient (Dinkelaker et al., 1995; Neumann et al., 1995; Keerthisinghe et al., 1998). Keerthisinghe and co-workers (1998) collected exudates along a proteoid root axis of white lupin and found that most of the efflux occurred in the youngest portion of the root axis, where the rootlets were young, and that the *in vitro* activities of PEPC and malate dehydrogenase were not strictly correlated with citrate fluxes from the same portion of root. The transition from primordial tissue to fully differentiated, determinate root tissue during rootlet growth suggests that enzymatic changes associated with development could be

¹ This study was funded in part by an Overseas Postgraduate Award to M.W. from the Australian Government.

* Corresponding author; e-mail evans@rsbs.anu.edu.au; fax 61-2-6249-4919.

Abbreviation: PEPC, PEP carboxylase.

confused with those associated with exudation and, as suggested by Dinkelaker et al. (1995), elucidation of the mechanisms related to exudation requires a detailed time-course study of rootlets of different ages. To our knowledge, there have been no such studies linking anatomical changes with biochemical changes and the efflux of organic acids on the proteoid rootlets of any species.

In the present study, we applied the root-incubation chamber used by Keerthisinghe et al. (1998) to study proteoid rootlets of white lupin from the time of emergence through d 8. Our first objective was to resolve the developmental and metabolic stages associated with efflux of organic acids by performing a detailed time-course study of rootlet anatomy and biochemistry for plants grown with low phosphorus and ambient atmospheric [CO₂].

Increases in atmospheric [CO₂] can alter root growth and turnover (for review, see Rogers et al., 1994; for example, see Fitter et al., 1996) and can increase the amount of carbon-containing compounds exported to the rhizosphere (Paterson et al., 1997). However, there have been few studies measuring the quantity and quality of exudates on a per-root basis under ambient and elevated [CO₂] (Sadowsky and Schortemeyer, 1997), particularly those exudates that function in nutrient acquisition, such as organic acids. If such exudates are increased under elevated atmospheric CO₂, they may confer an advantage to those species with these processes (Gifford et al., 1996; DeLucia et al., 1997). Because white lupin exports a large amount of carbon as citrate from proteoid lateral roots with defined, determinate development, they are an ideal system with which to study the effects of atmospheric [CO₂] on root and exudate processes. Our second objective was to investigate the effect of atmospheric [CO₂] on proteoid root growth, development, and efflux.

MATERIALS AND METHODS

Plant Growth

White lupin (*Lupinus albus* L. cv Kiev mutant) was grown in ambient (350 $\mu\text{L L}^{-1}$) or elevated (700 $\mu\text{L L}^{-1}$) atmospheric CO₂ in climate-controlled growth cabinets with a 12-h photoperiod, 600 $\mu\text{mol m}^{-2} \text{s}^{-1}$ light at leaf level, 70% RH, and 15°C/22°C night/day temperatures. Seeds were germinated in damp sand and at d 6 (2 d after cotyledon emergence) were transferred to black, 22-L hydroponics tanks. Four seedlings per tank were supported by removable foam discs that fit into the lid. Each tank contained a solution of 1 μM KH₂PO₄, 0.25 mM CaCl₂, 0.7 mM KNO₃, 0.25 mM MgSO₄, 11 μM H₃BO₃, 2 μM MnSO₄, 0.35 μM ZnSO₄, 0.2 μM CuSO₄, and 6 μM ferric EDTA and was adjusted daily to pH 6.0 (Keerthisinghe et al., 1998). Each day, phosphate levels were assayed using Malachite green dye and replenished to 1 μM (Irving and McLaughlin, 1990; Keerthisinghe et al., 1998). The complete solution in the tanks was changed weekly or biweekly. Preliminary experiments indicated that nitrate had been depleted by less than 20% between solution changes. The nutrient solution was aerated continuously from rings with small perforations supported at the bottom of the tanks.

Scoring Proteoid Root Development

The working definition of a proteoid root was a primary lateral root with defined clusters of more than 10 secondary lateral roots (proteoid rootlets) per centimeter (Figs. 1 and 3; Johnson et al., 1996b). The emergence of these clusters of proteoid rootlets was scored daily for 3 to 4 weeks by removing a plant from the hydroponics tank, spreading the root system in a shallow dish of water, and counting clusters that had recently emerged from the root cortex (rootlets 0.5–1.0 mm long).

In Situ Collection of Root Exudates

Exudates were collected from incubated clusters of proteoid rootlets attached to the plant in their growing environments (Ryan et al., 1993; Keerthisinghe et al., 1998, see figure 1 therein). Plants were transferred to tanks partially filled with nutrient solution and the proteoid roots were supported on trays in the tanks. A Perspex resin incubation ring, 2 cm in diameter and 1.2 cm in height, with two small notches to fit over the axis of the lateral root, was sealed around a cluster of developing rootlets with silicon grease. Nutrient solution (2 mL) was placed around the isolated cluster and the tank was filled to cover the rest of the root system. In all experiments the solution in the ring was replaced every 6, 12, or 18 h with fresh nutrient solution. Keerthisinghe et al. (1998) reported that degradation of citrate did not occur in the incubation rings, so no precautions were taken to prevent the breakdown of organic acids during exudate collection in the experiments reported here. Any breakdown would have resulted in an underestimation of exported organic acids. Once collected from the rings, the solutions with the exudates were immediately frozen and stored at –20°C until organic acid analysis.

Exudates were collected from the fourth cluster of proteoid rootlets developing on the basal laterals on both ambient- and elevated-[CO₂]-grown plants when the plants were 26 d old (Figs. 2 and 3). In one experiment plants were grown with either ambient or elevated [CO₂], and exudates were collected continuously for 6 to 8 d, from the time that the rootlets emerged from the cortex and were 0.5 to 1 mm long (Fig. 3B). The cluster was photographed daily in the incubation ring for correlation of rootlet growth with exudate efflux. Rootlet length was measured directly from photographs using a digitizing tablet. Eight rootlets per cluster and 12 clusters from four plants per CO₂ treatment were measured.

In the second experiment plants were grown with ambient [CO₂] only. After the developmental time course shown in Figure 3B, exudates were collected for 24 h, and then the cluster was harvested. A sample of two to three rootlets plus approximately 1 mm of the adjoining main axis was excised from each harvested cluster and immediately fixed in glutaraldehyde on ice for anatomical studies. The remaining tissue was immediately frozen in liquid nitrogen for enzymatic studies.

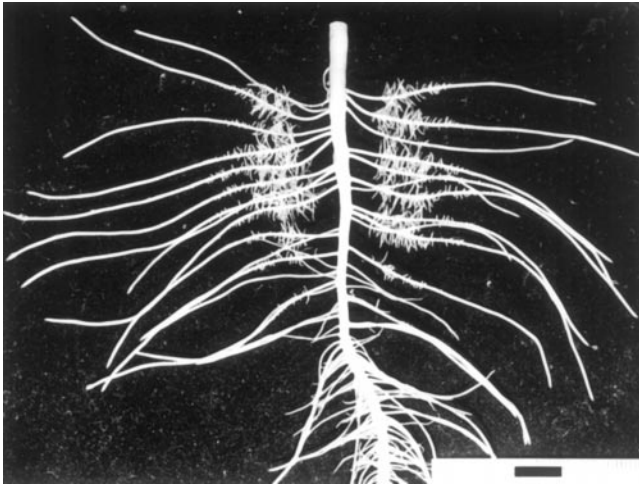


Figure 1. Root system of an 18-d-old white lupin plant germinated on sand for 6 d and then transferred to nutrient culture with $1 \mu\text{M}$ phosphorus and $350 \mu\text{L L}^{-1}$ atmospheric $[\text{CO}_2]$. All of the primary basal laterals have become proteoid roots and the first cluster of secondary laterals (proteoid rootlets) has fully emerged. The basal laterals are longer and thicker than the thinner, shorter, acropetal primary laterals. Scale bar = 1 cm.

Analysis of Exudates

Enzyme Assay for Citrate

Glycylglycine buffer (100 mM with 0.2 mM ZnCl_2 , pH 7.9), 0.3 mM NADH, 600 kilounits L^{-1} lactate dehydrogenase (EC 1.1.2.3), and 600 kilounits L^{-1} malate dehydrogenase were combined with 1 mL of thawed exudate, mixed thoroughly, and read at 340 nm in a spectrophotometer. Citrate lyase (EC 4.1.3.6) was added (final activity in cuvette 40 kilounits L^{-1}), and the absorbance was monitored until it stabilized. The decrease in absorbance was proportional and stoichiometric to the amount of citrate present in the reaction (Möllering, 1985; Keerthisinghe et al., 1998).

HPLC for Organic Acids

Exudates were thawed and 1 mL was passed through a $0.45\text{-}\mu\text{m}$ pore-size filter with a syringe. The filtrate was evaporated to dryness in a freeze drier (Speed Vac, Savant Instruments, Holbrook, NY), redissolved with 40 to $100 \mu\text{L}$ of 13 mM H_2SO_4 , and spun at 13,000 rpm for 5 min. Twenty-five microliters of the supernatant was injected into an HPLC (model 1090M, Hewlett-Packard) that was fitted with an ion-exclusion column (300×7.8 mm; HPX-87H Aminex, Bio-Rad) and an organic acid guard column (Bio-Rad). The mobile phase was 13 mM H_2SO_4 run at 0.5 mL min^{-1} at 60°C . The acids were detected at 210 nm with a photodiode-array UV detector. Standards for oxalic acid, citric acid, α -ketoglutaric acid, malic acid, succinic acid, pyruvic acid, and fumaric acid were made in distilled water at concentrations within the ranges found in the exudates. As with the samples, the standards were filtered, evaporated, suspended in 13 mM H_2SO_4 , centrifuged, and then run through the HPLC system individually or as a mixture. Linear standard curves were generated for each

acid from the areas under the peaks corresponding to different concentrations. The standard curves were used to quantify acids in the exudates. To verify running conditions, a mixture of the standard acids was run before each batch of samples was analyzed.

Specific Enzyme Activities and Protein Content

Each root sample was frozen, transferred to a chilled, 2-mL glass homogenizer, and ground on ice for 1 to 2 min in $250 \mu\text{L}$ of freshly prepared grinding solution (50 mM Hepes, 5 mM MgCl_2 , 1 mM EDTA, 1 mM EGTA, 0.1% Triton X-100, 10% glycerol, 0.5 mM PMSF dissolved in isopropanol, 5 mM DTT, 2 mM benzamidine, and 2 mM ϵ -amino-*n*-caproic acid). The ground sample was divided into three aliquots, snap-frozen in liquid nitrogen, and stored at -80°C until analysis. Just before analysis, samples were thawed on ice and centrifuged at 13,000 rpm for 10 min at 4°C ; the supernatant was maintained on ice.

PEPC activity in the tissue supernatant was measured by monitoring the oxidation of NADH at 340 nm in a spectrophotometer (Vance et al., 1983). The tissue supernatant ($40\text{--}80 \mu\text{L}$) was initially incubated for 10 min at 25°C in 100 mM Bicine, pH 8.0, with 5 mM MgCl_2 , 10 mM NaHCO_3 , 0.16 mM NADH, and 60 units of malate dehydrogenase. Next, $15 \mu\text{L}$ of 100 mM PEP was added and the decrease in absorbance per unit of time was measured.

Citrate synthase (EC 4.1.3.7) activity was measured by following the rate of 3-acetylpyridine adenine dinucleotide reduction at 365 nm in a spectrophotometer (Stitt, 1983). Tissue supernatant ($60\text{--}100 \mu\text{L}$) was incubated with 100 mM triethanolamine, pH 8.5, 3.5 mM malate, 0.3 mM 3-acetylpyridine adenine dinucleotide, and 30 units of malate dehydrogenase at 25°C until the absorbance had stabilized (approximately 15 min). Next, $15 \mu\text{L}$ of 10 mM acetyl-CoA was added and the increase in absorbance per unit of time was measured. Protein in the tissue supernatant was estimated using the Coomassie Plus protein assay reagent kit (Pierce).

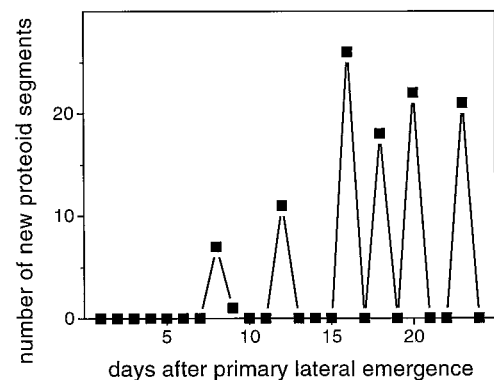


Figure 2. Emergence of clusters of proteoid rootlets scored daily on a white lupin plant grown in nutrient solution with $1 \mu\text{M}$ phosphorus and $350 \mu\text{L L}^{-1}$ atmospheric $[\text{CO}_2]$. Newly formed clusters emerged simultaneously in discrete pulses on all of the proteoid roots of the root system. The plot is of one representative plant; eight other plants exhibited similar patterns of cluster emergence. The primary laterals emerged when seedlings were 8 d old.

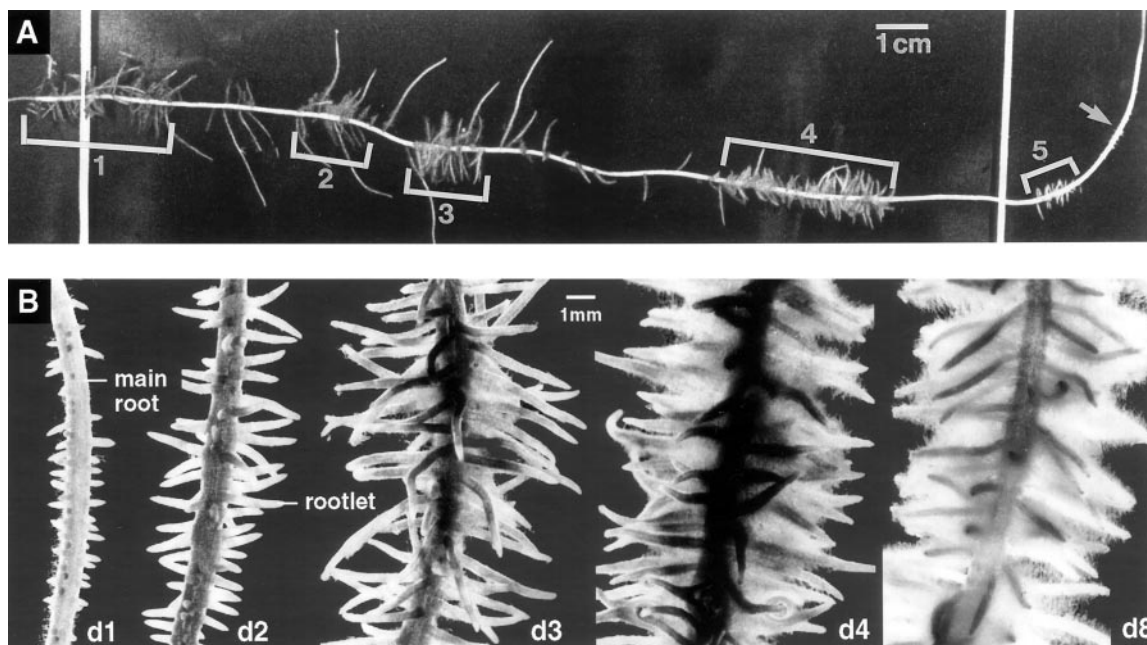


Figure 3. Clusters of rootlets along proteoid roots of white lupin grown in nutrient solution with $1 \mu\text{M}$ phosphorus and $350 \mu\text{L L}^{-1}$ atmospheric $[\text{CO}_2]$. A cluster is defined as a length of root with more than 10 rootlets per centimeter that have emerged in near synchrony. A, Proteoid root of a 32-d-old plant. Clusters of emerged rootlets are numbered. Studies relating development with citrate efflux were done on the fourth cluster of rootlets. Arrow indicates the sixth cluster. B, Developmental series of a proteoid root cluster. Rootlets emerged in near synchrony on d 1 and developed to similar final lengths of approximately 4 mm on d 4.

Tissue Preservation and Staining for Anatomy

Rootlets were fixed in 3% glutaraldehyde in 25 mM potassium-phosphate buffer, pH 6.8, on ice overnight, rinsed four times for 15 min each in buffer, postfixed in 1% osmium tetroxide for 2 h, and rinsed three times for 15 min each in buffer. The tissue was taken through a gradual dehydration series from 4% to 100% ethanol over 2 d on ice and then at room temperature and slowly infiltrated with Spurr's resin starting with 2.5% in ethanol and reaching 100% in 2 d. The Spurr's resin was replaced daily for 5 d and then the resin-embedded tissue was polymerized at 70°C overnight.

Transverse and longitudinal sections ($2\text{--}3 \mu\text{m}$ thick) of resin-embedded material were cut with a glass knife, transferred to drops of water on gelatin-coated glass slides, and dried on a hot plate for 1 h. Sections were first stained with 1% toluidine blue in borate, pH 11.0, and viewed with bright-field optics to show general anatomy and development. To visualize phloem differentiation, the resin was etched from the sections with sodium ethoxide (1–2 min), rinsed with 70% ethanol, and then rinsed for 1 min in running tap water. The sections were then stained with Schiff's reagent for 4 min to reduce background wall autofluorescence, rinsed for 5 min in running tap water, and stained with 0.05% aniline blue in 67 mM potassium-phosphate buffer, pH 8.6, for 2 h. Sections were mounted

in fresh aniline blue and viewed with UV fluorescence optics (Axioplan microscope, Zeiss). The callose deposited in the walls and plates of the sieve tubes fluoresces bright blue/green and could therefore be distinguished from lignin and suberin autofluorescence (O'Brien and McCully, 1981).

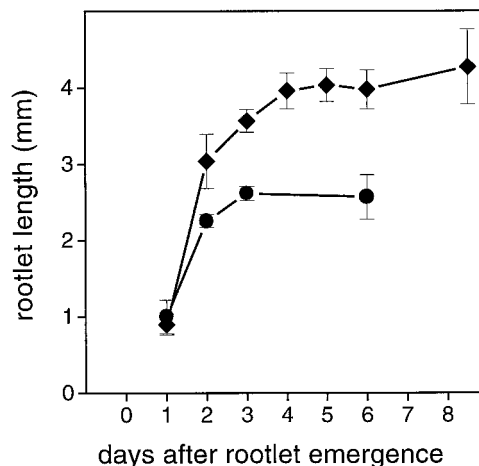


Figure 4. Lengths of proteoid rootlets of white lupin grown in nutrient culture with $1 \mu\text{M}$ phosphorus. Rootlets grown with $700 \mu\text{L L}^{-1}$ atmospheric $[\text{CO}_2]$ (●) reached a shorter final length 1 d earlier than rootlets grown with $350 \mu\text{L L}^{-1}$ atmospheric CO_2 (◆). Each point represents the mean \pm SE of 12 roots from four plants per CO_2 treatment.

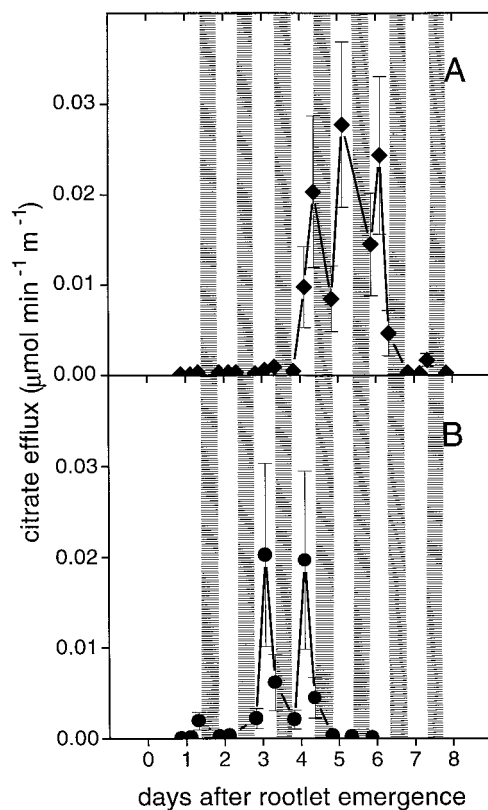


Figure 5. Citrate efflux from developing clusters of proteoid roots of white lupin grown in nutrient culture with $1 \mu\text{M}$ phosphorus. Shading indicates dark periods. Each point represents the mean \pm SE of 12 roots from four plants per CO_2 treatment. A, Plants grown with $350 \mu\text{L L}^{-1}$ atmospheric $[\text{CO}_2]$. Citrate efflux began 4 d after rootlet emergence, when rootlets had stopped elongating, and lasted 3 d, with strong peaks during light periods. B, Plants grown with $700 \mu\text{L L}^{-1}$ atmospheric $[\text{CO}_2]$. Citrate efflux began 3 d after rootlet emergence when rootlets had stopped elongating and lasted 2 d with strong peaks during light periods.

RESULTS

Root System Architecture and Proteoid Root Morphology

We found in white lupin a taproot system with approximately 20 thick, indeterminate, basal primary laterals in addition to the thinner, shorter, acropetal primary laterals (Fig. 1). All of the basal primary laterals became proteoid roots, developing distinct clusters of closely spaced, determinate, secondary laterals or proteoid rootlets. Few of the thinner, acropetal laterals became proteoid roots as the plant aged. The clusters of proteoid rootlets emerged in near synchrony on all of the proteoid roots of the root system, regardless of root length (Fig. 2). The emergence of the first cluster of rootlets was predictable, occurring 7 d after the emergence of the basal laterals when the plant was approximately 2 weeks old. This first cluster often appeared on 7 to 15 basal primary laterals; the second and third clusters recruited more basal laterals. By the third cluster, a plateau was reached in the number of primary laterals becoming proteoid roots (Fig. 2).

An example of a basal primary lateral from a 32-d-old plant is shown in Figure 3A. Five root clusters are shown, with a sixth cluster just emerging from the cortex. The length and spacing of the root axis of each cluster varied; for the earlier clusters the morphology was more variable. For this study, all data were collected from the fourth cluster. A time course of rootlet development of this cluster is shown in Figure 3B. Within a cluster, almost all rootlets emerged from the cortex in near synchrony; they grew and developed at similar rates, with an occasional rootlet reaching 2 to 3 times the length of other rootlets.

Effect of Atmospheric $[\text{CO}_2]$ on Proteoid Rootlet Elongation and Efflux of Organic Acids

Rootlet length was measured on clusters restrained in the incubation rings. Rootlets grew rapidly for the first 2 d, reaching their final 4-mm length 4 d after emergence from

Table 1. Rates of efflux of organic acids detected around proteoid roots before, during, and after peaks in efflux activity

Plants were grown with ambient ($350 \mu\text{L L}^{-1}$) or elevated ($700 \mu\text{L L}^{-1}$) atmospheric $[\text{CO}_2]$, and exudates were collected in situ with incubation rings on roots for 1 week. Each value represents the mean \pm SE of exudates from one root from each of three to six plants.

Organic Acid	Efflux Rate					
	Ambient $[\text{CO}_2]$			Elevated $[\text{CO}_2]$		
	Prepeak	Peak	Postpeak	Prepeak	Peak	Postpeak
	<i>nmol min⁻¹ m⁻¹</i>					
Enzymatic analysis						
Citrate	0.27 ± 0.22	23 ± 7	ND ^a	0.19 ± 0.11	19 ± 3	ND
HPLC analysis						
Citrate	ND	33 ± 10	0.29 ± 0.29	ND	23 ± 4	0.1 ± 0.04
Oxalate	1.2 ± 0.2	0.019 ± 0.019	0.3 ± 0.03	0.8 ± 0.15	0.7 ± 0.31	0.23 ± 0.02
α -Ketoglutarate	0.082 ± 0.044	0.055 ± 0.055	0.11 ± 0.09	0.07 ± 0.04	0.17 ± 0.11	0.004 ± 0.004
Malate	1.4 ± 0.78	0.55 ± 0.25	0.34 ± 0.12	0.35 ± 0.19	0.43 ± 0.16	0.13 ± 0.04
Succinate	0.069 ± 0.069	0.042 ± 0.042	ND	0.83 ± 0.48	0.87 ± 0.42	0.17 ± 0.12
Pyruvate	0.81 ± 0.52	ND	1.18 ± 0.8	0.49 ± 0.3	0.043 ± 0.043	0.05 ± 0.05
Fumarate	0.12 ± 0.12	ND	0.12 ± 0.05	0.31 ± 0.2	0.043 ± 0.036	0.09 ± 0.07
Total ^b	3.6 ± 1.3	34 ± 10	2.3 ± 0.68	2.86 ± 0.57	26 ± 4	0.75 ± 0.09

^a ND, Not detected.

^b Sum of all organic acids detected by HPLC.

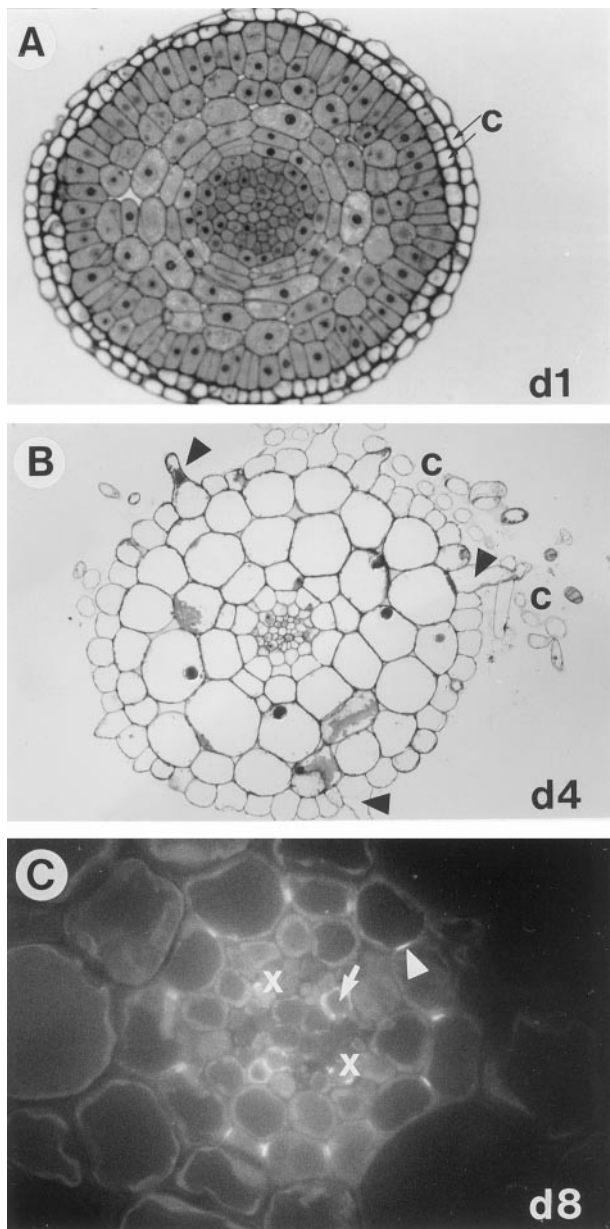


Figure 6. Cross-sections (3 μm thick) through the tips of resin-embedded proteoid rootlets of white lupin grown in nutrient culture with 1 μM phosphorus and 350 $\mu\text{L L}^{-1}$ atmospheric $[\text{CO}_2]$. A, Rootlet 1 d after emergence from the cortex of the proteoid root. All of the cells shown are meristematic except for the root-cap cells, which are tightly anchored to the epidermis. Magnification = $\times 280$. B, Rootlet 4 d after emergence from the cortex. The apical meristem is no longer present and all cells in the rootlet have vacuolated and differentiated. The epidermis has differentiated root hairs to the tip of the rootlet, and the root-cap cells are loosely anchored. Magnification = $\times 300$. C, Rootlet 8 d after emergence from the cortex. The stele has two xylem and two phloem poles and is surrounded by an endodermis with a Casparian band. Sections from d 1 and 4 were stained with toluidine blue and viewed with bright-field optics. The section from d 8 was etched after sectioning to remove the resin, stained with Schiff's reagent, mounted in aniline blue, and viewed with fluorescence optics. Black arrowheads, Root hairs; white arrowheads, Casparian bands; white arrow, phloem sieve tube; x, xylem vessel. Magnification = $\times 1000$.

the cortex in plants grown with ambient $[\text{CO}_2]$ (Fig. 4). Elevated atmospheric $[\text{CO}_2]$ resulted in the rootlets stopping growth after only 3 d, reaching only a 2.5-mm final length.

At both CO_2 concentrations, the onset of citrate efflux occurred after the rootlets stopped elongating; onset was 1 d earlier in plants grown with elevated atmospheric $[\text{CO}_2]$ (Fig. 5). Citrate efflux continued for 2 d in the elevated- $[\text{CO}_2]$ -grown plants and for 3 d in the ambient- $[\text{CO}_2]$ -grown plants. Peaks in efflux occurred during the day under both CO_2 treatments, and the peak efflux rate per unit of length of proteoid root was not altered by atmospheric $[\text{CO}_2]$. Citrate was the dominant organic acid exuded from the roots, being 60-fold higher than malate at peak efflux of citrate (Table I). Other organic acids were detected at very low concentrations and were unaffected by the atmospheric $[\text{CO}_2]$.

Rootlet Development and Anatomy

The development and anatomy of the proteoid rootlets are illustrated in Figures 6 and 7 and summarized in Table II. One day after emergence from the proteoid root, the rootlets were almost entirely meristematic (Figs. 6A and 7F); only the cells of the rootlet cortex within the proteoid root had started to vacuolate and elongate. The phloem sieve tubes were visible at approximately six cell lengths from the phloem of the stele of the proteoid root axis, and extended over only 25% of the rootlet length. The root cap adhered tightly to the rootlet tip; at this stage no root hairs had developed. On d 2, many rootlet cells were developing vacuoles and elongating, whereas cells toward the tip of the stele and cortex still had high amounts of cytoplasm (Fig. 7G). Root hairs were beginning to develop; root-cap cells were sloughing from the epidermis and could be seen along the length of the rootlet; and callose in the phloem sieve tubes had differentiated along 60% of the rootlet length (Fig. 7, G and L).

By d 3, rootlets were approaching their final length (Fig. 4), all cells had vacuolated, and the apical meristem was no longer present. Root hairs were long and dense toward the base of the rootlet, and epidermal cells around the tip were just developing hairs (Fig. 7, C and H). The distribution of root-hair growth along the rootlet varied, however, with some rootlets showing very dense proliferation toward the tip and others toward the base. The phloem sieve tubes and protoxylem secondary walls were visible to within five cell lengths of the rootlet tip, indicating that the stele had differentiated along more than 95% of the rootlet length (Fig. 7H).

By d 4, citrate efflux had started (Fig. 5A) and root hairs continued to expand (Fig. 7D). The root cap was loosely anchored and sloughed clumps of root-cap cells were often associated with root hairs (Figs. 6B and 7I). Rootlet development from d 5 to 8 was similar to that seen at d 4, although root hairs continued to develop until d 6. A completely differentiated rootlet had sloughed root-cap cells and an epidermal layer with root hairs had differentiated around the tip of the rootlet. Four layers of cortical

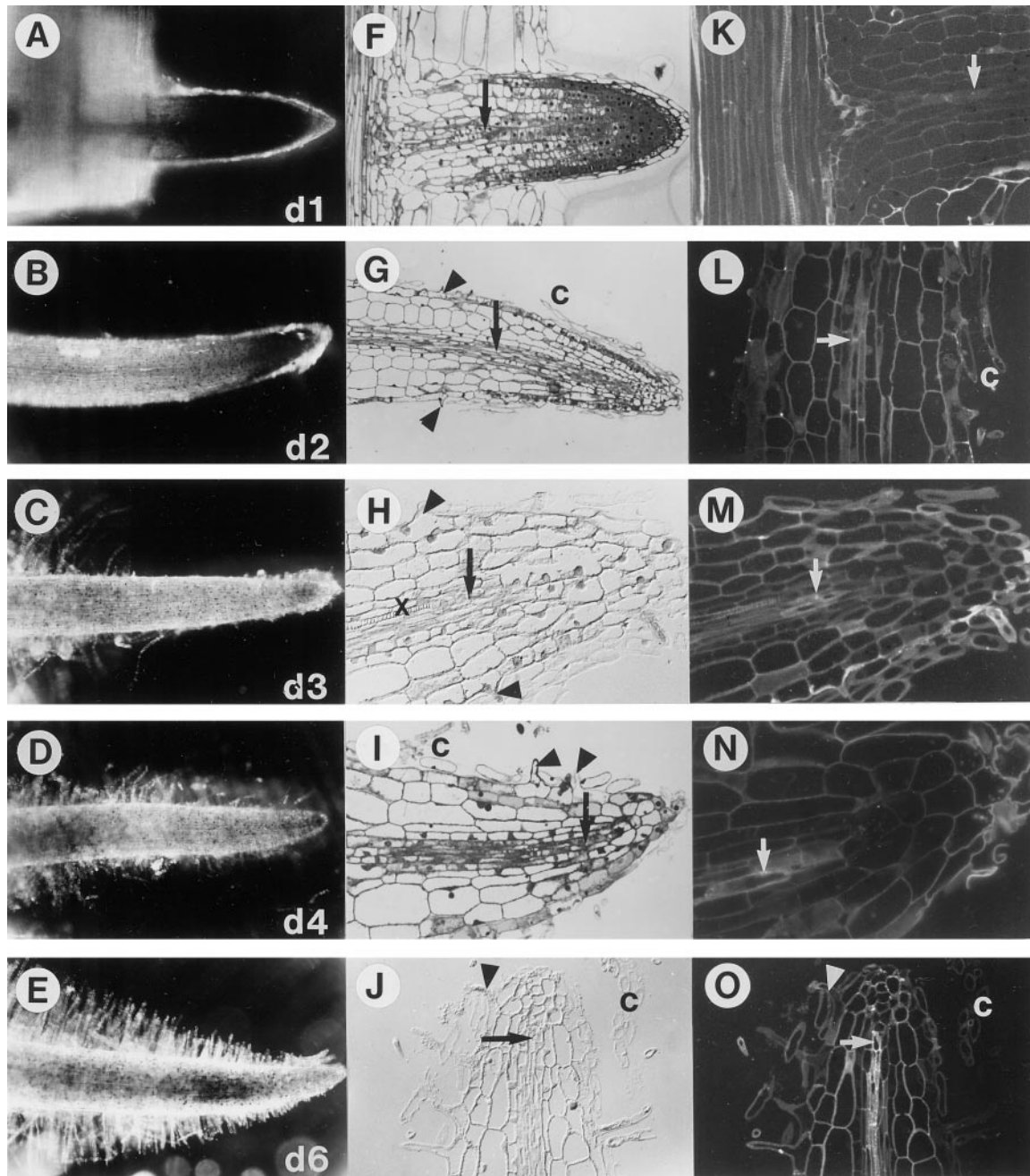


Figure 7. Development from 1 d after emergence from the cortex of proteoid rootlets from white lupin grown in nutrient culture with $1 \mu\text{M}$ phosphorus and $350 \mu\text{L L}^{-1}$ atmospheric $[\text{CO}_2]$. Left, Whole mounts of glutaraldehyde- and osmium-fixed rootlets embedded in resin. Center, Longitudinal sections ($3 \mu\text{m}$ thick) through rootlets shown at left stained with toluidine blue (F, G, and I) or left unstained and viewed with differential image contrast bright-field optics (H and J). Right, Longitudinal sections ($3 \mu\text{m}$ thick) etched to remove resin, stained with Schiff's reagent followed by aniline blue, and viewed with UV fluorescence optics. Arrows, Points of visible callose deposition in the phloem; x, xylem secondary wall; arrowheads, root hairs; c, root cap. At d 1, rootlets are almost entirely meristematic. At d 2, most of the cells are developing vacuoles, root hairs have started to develop at the base, and the phloem callose extends to 75% of the rootlet length. At d 3, the apical meristem is completely exhausted, and root hairs and vascular tissues have differentiated along the length of the rootlet. Days 4 and 6 are similar to d 3. Refer to text for more details. Rootlet diameter was approximately $225 \mu\text{m}$. Magnification: A to E, $\times 60$; F and G, $\times 100$; H and M, $\times 180$; I, J, L, and O, $\times 170$; K, $\times 150$; and N, $\times 425$. The root tip in L, J, and O is pointing up.

cells (the innermost being an endodermal layer with a suberized Casparian band) are shown in Figure 6C, and a

section) is shown in Figure 6B. The stele had two phloem poles and two protoxylem poles (with spiral secondary wall thickenings; Figs. 6C and 7H).

Table II. Development and citrate efflux of proteoid rootlets, ranging from none detected (–) to maximum (+++), in plants grown with ambient $[CO_2]$

Rootlet Age	Development			Citrate Efflux
	Meristematic cells	Phloem and xylem	Root hairs	
d				
1	+++	+	–	–
2	++	++	+	–
3	–	+++	++	–
4	–	+++	+++	++
5	–	+++	+++	+++
6	–	+++	+++	++
7-8	–	+++	+++	–

The dry weight of clusters of rootlets increased between d 1 and 5, plateaued, and then dropped at d 8 (Fig. 8A). Fresh weight increased abruptly on d 3 and 4 because of root-hair development and vacuolation of cells (Fig. 8B); as a consequence, the soluble protein content per unit of fresh weight fell sharply (Fig. 8C). The soluble protein content per unit of root length increased steadily to a peak on d 3 before declining again (Fig. 9C).

Enzyme Activities and Citrate Efflux

In vitro PEPC activity per unit of protein peaked 3 d after rootlet emergence, doubling in activity between d 1 and 3 before decreasing to 25% of peak activity by d 8 (Fig. 9A). Citrate synthase activity per unit of protein declined by 50% on d 1, after which it plateaued for 5 d before declining again (Fig. 9B).

Both PEPC and citrate synthase had maximal activity per unit length of proteoid root 3 d after rootlet emergence, preceding the onset of citrate efflux by 1 d and the peak of efflux by 2 d (Fig. 10). PEPC and citrate synthase had approximately 4- and 3-fold increases in activity, respectively, between d 1 and 3. Citrate efflux from the developmental time-course samples that were harvested daily lasted 3 d, with efflux peaks during photoperiods (Fig. 10C). This length of time was similar to that of the efflux from developing roots maintained in the incubation rings for 8 d (Fig. 5A); however, efflux from roots collected from rings in place for just 24 h was twice that of the roots maintained in rings for 8 d. The total amount of citrate exudation was equivalent to 10% of the proteoid-root dry weight. In vitro activities of PEPC and citrate synthase were well in excess of citrate-exudation rates at all times.

DISCUSSION

Synchronous Development of Proteoid Roots

A striking finding of this study was the predictable and synchronous development of clusters of rootlets on the proteoid roots in white lupin grown in solution culture (Fig. 2). This implicates a central signaling cascade for development of clusters of rootlets. Studies showing that the internal phosphorus status of the plant can determine proteoid root development in white lupin (Marschner et

al., 1987; Keerthisinghe et al., 1998) and wax myrtle (Louis et al., 1990) support a central signaling mechanism. The signal may start in the shoot and radiate down to the roots, reaching the basal laterals first. It is possible that the signaling process is delivered to the roots in pulses related to the plant phosphorus status, if so, the frequency and duration would determine the spacing and length of each cluster of rootlets along the proteoid root axis. As the severity of phosphorus stress grew, signaling would intensify, thus increasing the proportion of the root system covered with proteoid rootlets (Keerthisinghe et al., 1998).

The signals involved in proteoid root development probably include auxin. Gilbert et al. (1997) were able to use auxin to induce the production of proteoid rootlets in white lupin when phosphorus was supplied at a level that normally suppresses their development, and they could sup-

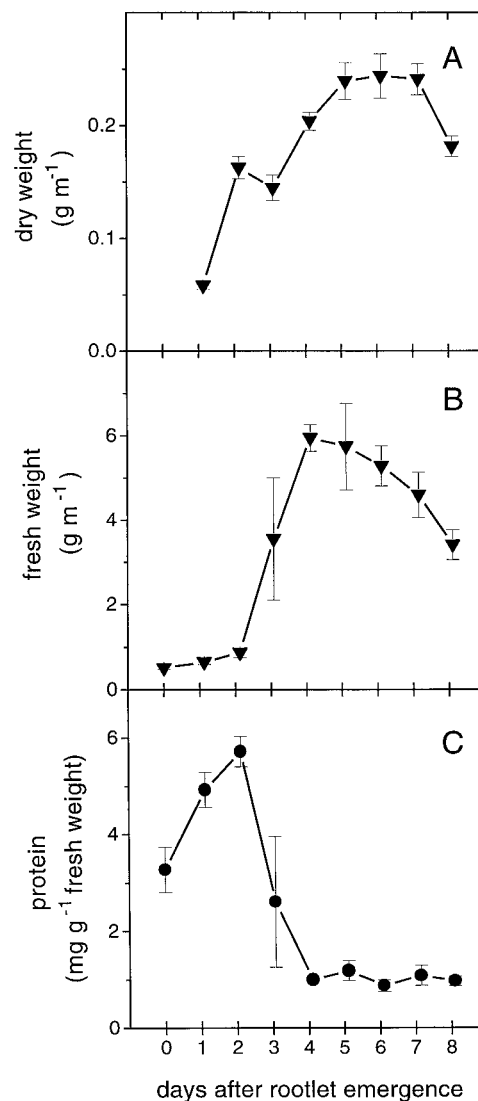


Figure 8. Dry weight (A), fresh weight (B), and soluble protein content (C) of proteoid root clusters of white lupin grown in nutrient culture with $1 \mu M$ phosphorus and $350 \mu L L^{-1}$ atmospheric $[CO_2]$. Each point represents the mean \pm SE of one root from each of four to six plants.

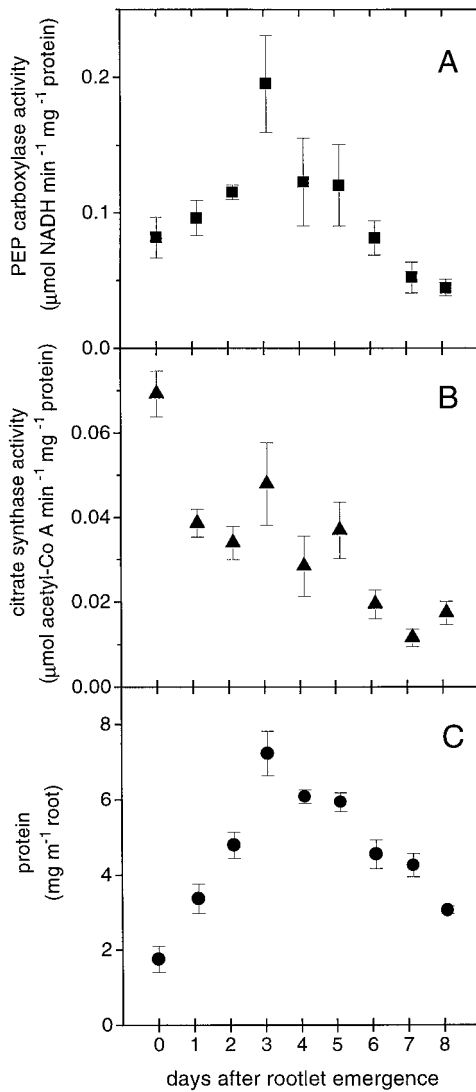


Figure 9. In vitro PEPC (A) and citrate synthase activities (B) per unit of soluble protein of developing proteoid root clusters from white lupin grown in nutrient culture with 1 μM phosphorus and 350 $\mu\text{L L}^{-1}$ atmospheric $[\text{CO}_2]$. C, Soluble protein peaks 3 d after rootlet emergence. Each point represents the mean \pm SE of one root from each of four to six plants.

press proteoid rootlet formation in minus-phosphorus treatments by supplying auxin-transport inhibitors to the nutrient solution. Auxin plays a role in lateral root initiation in other species (Thimann, 1936; Wightman et al., 1980); in the *Arabidopsis* mutant, *superroot* is responsible for a phenotype that is very similar to a proteoid root (Boerjan et al., 1995).

The rootlets that developed within clusters along a proteoid root reached a similar, determinate length, although an occasional rootlet extended two to three times the length of the other rootlets (Fig. 3A). Determinacy has been reported in all species that form proteoid roots (Dinkelaker et al., 1995) but has also been observed in roots from other types of species (Varney and McCully, 1991; Dubrovsky, 1997). The average final length of a rootlet varies within

and among proteoid species; recently Skene et al. (1998a) showed that rootlets of *Grevillea robusta* were shorter when they developed in hydroponics compared with development in vermiculite. To our knowledge, we are the first to report that determinacy varies with environmental treatment ($[\text{CO}_2]$) in a common rooting medium (Fig. 4), indicating that root determinacy is under internal control. Controls for root determinacy are unknown, but the switch from indeterminacy to determinacy in stem nodules has been linked to the environment and the presence of the hormone ethylene (Fernández-López et al., 1998). Although auxin is responsible for initiating lateral root growth, continued exposure to auxins can inhibit elongation of laterals (Thimann, 1936). In addition, cytokinins have been shown to suppress lateral root formation (Wightman et al., 1980). The effects of cytokinins or ethylene on proteoid root development are not yet known.

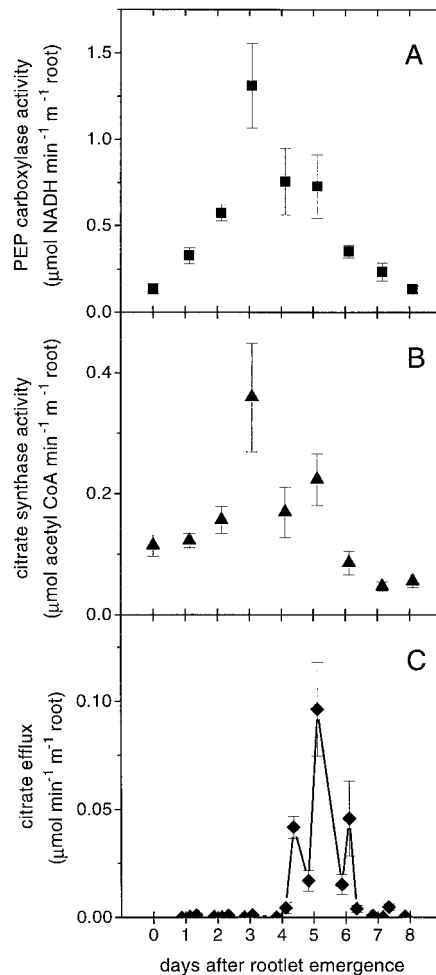


Figure 10. In vitro PEPC activity (A), citrate synthase activity (B), and citrate efflux (C) per unit length of white lupin proteoid root grown in nutrient culture with 1 μM phosphorus and 350 $\mu\text{L L}^{-1}$ atmospheric $[\text{CO}_2]$. PEPC and citrate synthase activities per unit length of main root peaked 3 d after rootlet emergence, 1 d before onset of citrate efflux and 2 d before the peak in citrate efflux on d 5. Each point represents the mean \pm SE of one root from each of four to six plants.

Rootlet Development and Citrate Efflux

The anatomy of white lupin proteoid rootlets is similar in most respects to that of members of the Proteaceae, in which the mature rootlets have a differentiated apex, root hairs to the tip, a loosely anchored root cap, an endodermis with a Casparian band, and a diarch stele (for review, see Dinkelaker et al., 1995; Skene et al., 1998b). Root-hair development in white lupin differs from that of *G. robusta* (Skene et al., 1996, 1998a) and *Hakea obliqua* (Dell et al., 1980). In *G. robusta*, root hairs were produced only after the rootlet had reached its final length; they then developed back from the tip. In *H. obliqua*, few hairs were produced in water culture, whereas they were produced extensively in soil.

Citrate efflux began shortly after the rootlets reached their final length. By that stage, phloem and xylem tissues had differentiated to the tips of the rootlets, enabling the import of photosynthates and the export of nutrients mobilized by the citrate exudation. Root hairs started to develop 2 d after emergence from the cortex, which was also 2 d before the onset of citrate efflux. This suggests that the presence of root hairs does not alone determine organic acid export.

Citrate export lasted only 2 to 3 d and then stopped. Neumann et al. (1995) also reported transient release of organic acids from a proteoid root cluster of *Hakea undulata*, although they did not document root development. Keerthisinghe et al. (1998) found that citrate efflux was maximal 1 to 3 cm from the tip and was only one-tenth that rate from either the 0- to 1-cm or the 5- to 9-cm region. The protein content of the rootlets peaked 3 d after emergence and then declined during citrate efflux (Fig. 9C). The links among determinacy, longevity, metabolism related to senescence, and efflux of organic acids remain to be investigated.

Some plants export organic anions from their roots upon exposure to Al; the organic acids chelate the Al, conferring tolerance. The fact that white lupin can export large amounts of citrate, an excellent chelator of Al, suggests that it may be tolerant to soils with high levels of available Al. However, citrate is not exported to the rhizosphere until the rootlets are fully mature, 2 to 4 d past the time that the rootlets are dividing and meristematic and are thought to be most susceptible to Al damage (Ryan et al., 1993). If the emerging rootlets are not protected from damage by exposure to Al, they will be hindered in their ability to access phosphorus when they are mature, imposing a double stress in very acidic soils. To confer Al tolerance, organic acid efflux from roots should coincide with the time that they are meristematic.

Enzyme Activities and Citrate Efflux

We did not find a correlation between PEPC activity and the magnitude of citrate efflux, because the peak in *in vitro* PEPC activity preceded the onset of citrate efflux by 1 d and preceded peak efflux by 2 d (Fig. 10). Furthermore, *in vitro* citrate synthase activity per unit of protein did not increase during citrate efflux, although citrate was the dominant organic acid exported. Our results contrast with

those of Johnson et al. (1994, 1996b), who suggested that increases in PEPC activity per unit of protein, as well as mRNA expression and abundance, coincide with organic acid efflux from the roots, and thus provide necessary carbons for the anapleurotic functioning of the tricarboxylic acid cycle during exudation. In the studies by Johnson et al. (1994, 1996b), enzyme activities were not measured on the same tissues from which exudates were collected; exudates were collected from the entire root system by flushing the pot with nutrient solution every 2 d, whereas enzyme activities were measured on root portions pooled from many plants. Although PEPC activity is clearly involved in citrate synthesis, it does not appear to determine the rate, onset, or duration of citrate exudation. Keerthisinghe et al. (1998) made concomitant measurements of citrate efflux and PEPC activity from 2-cm regions along a proteoid root axis and found that rates of citrate efflux did not vary proportionally with PEPC activity, which is in agreement with our findings.

In vitro activities of both PEPC and citrate synthase exceeded the rates of citrate exudation at every stage; however, these activities may not reflect the actual rates realized *in vivo*. The white lupin PEPC may be regulated by phosphorylation, similar to the regulation of PEPC in other species (for review, see Vidal and Chollet, 1997). Neumann et al. (1999) measured similar citrate concentrations (20 $\mu\text{mol g}^{-1}$ fresh weight) in juvenile, mature, and senescent proteoid root segments of white lupin, but significant citrate exudation was observed only in mature proteoid roots. Therefore, PEPC activity and tissue citrate concentration must not control the rate of citrate exudation.

We have made preliminary measurements of respiration rates of whole pieces of proteoid roots that greatly exceed the peak rate of exudation (4 $\mu\text{mol O}_2 \text{g}^{-1}$ dry weight min^{-1} for 0.025 $\mu\text{mol citrate g}^{-1}$ dry weight min^{-1}), suggesting that the flux through the TCA cycle is unlikely to limit the rate of citrate exudation. Neumann et al. (1999) measured similar respiration rates by mature and senescent proteoid root segments of white lupin, despite significant citrate exudation by mature but not senescent proteoid roots. Most of the respiration in hydroponically grown, mature proteoid roots is therefore involved in other metabolic processes such as ion uptake and amino acid synthesis (Jeschke and Pate, 1995; Johnson et al., 1996b) and maintenance rather than in citrate synthesis for exudation.

In the present study, there was a strong effect of day and night on citrate efflux, with peaks in efflux occurring during the light periods. To our knowledge, this is the first time a diurnal rhythm has been reported for organic acids exported from roots. A diurnal rhythm has been reported for the export of phyto siderophores from graminaceous roots in response to Fe deficiency (Ma and Nomoto, 1996). The highest tissue concentrations and effluxes of phyto siderophores also occur in the light, but it is unclear whether the mechanisms are directly linked to light or temperature (Ma and Nomoto, 1996).

Our data strongly suggest that citrate export is not simply a result of PEPC activity supplying the tricarboxylic acid cycle. Another key step must be regulating the export of citrate from the roots. In a study by Ryan et al. (1995),

neither malate dehydrogenase nor PEPC showed enhanced specific activities associated with malate efflux from wheat root tips. The same investigators showed that efflux of malate is likely to be linked to the activity of an anion transporter that was detected on the plasma membrane of the root tip cells (Ryan et al., 1997). The transport mechanism for organic acid efflux from proteoid roots is not known, although Dinkelaker et al. (1989) concluded that citrate is excreted concomitantly with protons. It seems likely that an anion transporter in the plasma membrane is synthesized and becomes active as rootlet elongation ceases. The transporter is then inactivated after 2 to 3 d, stopping further exudation. This transporter could be located in specific cells, but whether those are in the cortex, the epidermis, or elsewhere is unknown. Incubation of proteoid roots in solutions of anion-channel blockers reduced citrate exudation by 50% (Neumann et al., 1999), supporting the existence of an anion channel.

Effect of Elevated Atmospheric [CO₂]

Growth under elevated atmospheric [CO₂] altered the development of root clusters. Rootlets were shorter, reaching their final length and beginning citrate exudation 1 d earlier than ambient-[CO₂]-grown plants (Figs. 4 and 5). It is unclear how atmospheric [CO₂] alters rootlet determinacy. Atmospheric CO₂ can enhance lateral root turnover in some species and in certain soil environments (Pregitzer et al., 1995; Berntson and Bazzaz, 1996; Fitter et al., 1996) and may do so in proteoid rootlets by promoting exhaustion of the apical meristem and shortening growing time. By advancing the onset of determinacy and the onset of citrate efflux, residency time of a proteoid root cluster in a patch of soil may be decreased. In the present study, elevated atmospheric [CO₂] did not change the rate of citrate efflux or the composition of background organic acids per unit of length of proteoid root, although it did shorten the period over which this efflux occurred (Fig. 5). Unfortunately, the present experimental technique was not able to provide an integrated picture of efflux for a whole plant such as can be gained by the method of Johnson et al. (1996b).

There is a paucity of data regarding measurements of root exudation in the literature, but there is a great deal of speculation. The data shown in Figure 5 suggest that an increased efflux from roots under elevated atmospheric [CO₂] would occur if growth of the basal lateral roots were enhanced. However, given that the exudation pulse was shorter, this is by no means certain. The white lupin system illustrates the transient nature of exudation, its dependence on a specific stage of root development and time of day, and, even at peaks in efflux, the variability among samples from similar atmospheric CO₂ environments.

Whipps (1985) showed that carbon export per unit of length of maize root was unaltered by ambient CO₂ treatment. Similarly, Norby et al. (1987) concluded that there was no consistent effect of elevated [CO₂] on root exudation from pine seedlings, either per unit mass of fine root or as a percentage of photosynthate. Gifford et al. (1996), measuring citrate efflux per unit of dry weight of *Danthonia*

root tips, were unable to detect a significant difference among atmospheric CO₂ treatments, although exudation was consistently greater at elevated [CO₂]. DeLucia et al. (1997) detected an increase in oxalic acid in the rhizosphere of pine seedlings in response to increased atmospheric [CO₂]; however, these investigators did not measure efflux per unit of root length and did not differentiate between root-derived and hyphae-derived exudates. Using stable-isotope techniques, Hungate et al. (1997) showed that the total labile carbon pool, including root exudation and respiration, was larger in grassland growing with elevated atmospheric [CO₂].

In conclusion, with the limited amount of data available, it is not possible to conclude that elevated atmospheric [CO₂] alters the rate of carbon exudation from a given length of root. However, if root production were to be enhanced by elevated atmospheric [CO₂], then overall exudation could also be enhanced.

ACKNOWLEDGMENTS

We are grateful to Gamini Keerthisinghe (Commonwealth Scientific and Industrial Research Organization Plant Industry, Canberra, Australia) for help with establishing the hydroponics and exudate collection system and to Charlie Hocart (Research School of Biological Sciences, Australian National University) for help with the HPLC analyses.

Received November 24, 1998; accepted March 9, 1999.

LITERATURE CITED

- Berntson GM, Bazzaz FA (1996) The allometry of root production and loss in seedlings of *Acer rubrum* (Aceraceae) and *Betula papyrifera* (Betulaceae): implications for root dynamics in elevated CO₂. *Am J Bot* 83: 608–616
- Boerjan W, Cervera MT, Delarue M, Beekman T, Dewitte W, Bellini C, Caboche M, Van Onckelen H, Van Montagu M, Inzé D (1995) *superroot*, a recessive mutation in *Arabidopsis*, confers auxin overproduction. *Plant Cell* 7: 1405–1419
- Dell B, Kuo J, Thomson GJ (1980) Development of proteoid roots in *Hakea obliqua* R. Br. (Proteaceae) grown in water culture. *Aust J Bot* 28: 27–37
- DeLucia EH, Callaway RM, Thomas EM, Schlesinger WH (1997) Mechanisms of phosphorus acquisition for Ponderosa pine seedlings under high CO₂ and temperature. *Ann Bot* 79: 111–120
- Dinkelaker B, Hengeler C, Marschner H (1995) Distribution and function of proteoid roots and other root clusters. *Bot Acta* 108: 183–200
- Dinkelaker B, Römheld V, Marschner H (1989) Citric acid excretion and precipitation of calcium citrate in the rhizosphere of white lupin (*Lupinus albus* L.). *Plant Cell Environ* 12: 285–292
- Dubrovsky JG (1997) Determinate primary-root growth in seedlings of Sonoran desert Cactaceae: its organization, cellular basis, and ecological significance. *Planta* 203: 85–92
- Fernández-López M, Goormachtig S, Gao M, D'Haese W, Van Montagu M, Holsters M (1998) Ethylene-mediated phenotypic plasticity in root nodule development on *Sesbania rostrata*. *Proc Natl Acad Sci USA* 95: 12724–12728
- Fitter AH, Self GK, Wolfenden J, van Vuuren MMI, Brown TK, Williamson L, Graves JD, Robinson D (1996) Root production and mortality under elevated atmospheric carbon dioxide. *Plant Soil* 187: 299–306
- Gardner WK, Parbery DG, Barber DA (1981) Proteoid root morphology and function in *Lupinus albus*. *Plant Soil* 60: 143–147
- Gardner WK, Parbery DG, Barber DA (1983) The acquisition of phosphorus by *Lupinus albus* L. III. The probable mechanism by

- which phosphorus movement in the soil/root interface is enhanced. *Plant Soil* **70**: 107–124
- Gerke J, Römer W, Jungk A** (1994) The excretion of citric and malic acid by proteoid roots of *Lupinus albus* L.: effects on soil solution concentrations of phosphate, iron, and aluminum in the proteoid rhizosphere in samples of an oxisol and luvisol. *Z Pflanzenernähr Dueng Bodenkd* **157**: 289–294
- Gifford RM, Lutze JL, Barrett D** (1996) Global atmospheric change effects on terrestrial carbon sequestration: exploration with a global C- and N-cycle model (CQUESTN). *Plant Soil* **187**: 369–387
- Gilbert GA, Knight DJ, Vance CP, Allan DL** (1997) Does auxin play a role in the adaptations of white lupin roots to phosphate deficiency (abstract no. 67)? *Plant Physiol* **114**: S-31
- Hungate BA, Holland EA, Jackson RB, Chapin FS III, Mooney HA, Field CB** (1997) The fate of carbon in grasslands under carbon dioxide enrichment. *Nature* **388**: 576–579
- Irving GCJ, McLaughlin MJ** (1990) A rapid and simple field test for phosphorus in Olsen and Bray no. 1 extracts. *Commun Soil Sci Plant Anal* **21**: 2245–2255
- Jeschke WD, Pate JS** (1995) Mineral nutrition and transport in xylem and phloem of *Banksia prionotes* (Proteaceae), a tree with dimorphic root morphology. *J Exp Bot* **46**: 895–905
- Johnson JF, Allan DL, Vance CP** (1994) Phosphorus stress-induced proteoid roots show altered metabolism in *Lupinus albus*. *Plant Physiol* **104**: 657–665
- Johnson JF, Allan DL, Vance CP** (1996a) Root carbon dioxide fixation by phosphorus-deficient *Lupinus albus*. Contribution to organic acid exudation by proteoid roots. *Plant Physiol* **112**: 19–30
- Johnson JF, Allan DL, Vance CP** (1996b) Phosphorus deficiency in *Lupinus albus*. Altered lateral root development and enhanced expression of phosphoenolpyruvate carboxylase. *Plant Physiol* **112**: 31–41
- Keerthisinghe G, Hocking PJ, Ryan PR, Delaize E** (1998) Effect of phosphorus supply on the formation and function of proteoid roots of white lupin (*Lupinus albus* L.). *Plant Cell Environ* **21**: 467–478
- Lamont BB, Brown G, Mitchell DT** (1984) Structure, environmental effects on their formation, and function of proteoid roots in *Leucadendron laeololum* (Proteaceae). *New Phytol* **97**: 381–390
- Louis I, Racette S, Torrey JG** (1990) Occurrence of cluster roots on *Myrica cerifera* L. (Myricaceae) in water culture in relation to phosphorus nutrition. *New Phytol* **115**: 311–317
- Ma JF, Nomoto K** (1996) Effective regulation of iron acquisition in graminaceous plants: the role of mugineic acids as phytosiderophores. *Physiol Plant* **97**: 609–617
- Marschner H, Römheld V, Cakmak I** (1987) Root-induced changes of nutrient availability in the rhizosphere. *J Plant Nutr* **10**: 1175–1184
- Möllering H** (1985) Citrate. In HU Bergmeyer, ed, *Methods of Enzymatic Analyses*, Ed 3, Vol VII. VCH, Weinheim, Germany, pp 2–12
- Neumann G, Dinkelaker B, Marschner H** (1995) Kurzzeitige Abgabe organischer Säuren aus Proteoidwurzeln von *Hakea undulata* (Proteaceae). *Ökophysiologie des Wurzelraumes* **6**: 128–136
- Neumann G, Marsonneau A, Martinoia ER, Römheld V** (1999) Physiological adaptations to phosphorus deficiency during proteoid root development in white lupin. *Planta* (in press)
- Norby RJ, O'Neill EG, Hood WG, Luxmoore RJ** (1987) Carbon allocation, root exudation and mycorrhizal colonization of *Pinus echinata* seedlings grown under CO₂ enrichment. *Tree Physiol* **3**: 203–210
- O'Brien TP, McCully ME** (1981) *The Study of Plant Structure. Principles and Selected Methods*. Termarcarphi, Melbourne, Australia
- Paterson E, Hall JM, Rattray EAS, Griffiths BS, Ritz K, Killham K** (1997) Effect of elevated CO₂ on rhizosphere carbon flow and soil microbial processes. *Global Change Biol* **3**: 363–377
- Pregitzer KS, Zak DR, Curtis PS, Kubiske ME, Teeri JA, Vogel CS** (1995) Atmospheric CO₂, soil nitrogen and turnover of fine roots. *New Phytol* **129**: 579–585
- Purnell HM** (1960) *Studies of the family Proteaceae. I. Anatomy and morphology of the roots of some Victorian species*. *Aust J Bot* **8**: 38–50
- Rogers HH, Runion GB, Krupa SV** (1994) Plant responses to atmospheric CO₂ enrichment with emphasis on roots and the rhizosphere. *Environ Pollut* **83**: 155–189
- Ryan PR, Delhaize E, Randall PJ** (1995) Characterization of Al-stimulated efflux of malate from the apices of Al-tolerant wheat roots. *Planta* **196**: 103–110
- Ryan PR, DiTomaso JM, Kochian LV** (1993) Aluminum toxicity in roots: an investigation of spacial sensitivity and the role of the root cap. *J Exp Bot* **44**: 437–446
- Ryan PR, Skerrett M, Findlay GP, Delhaize E, Tyerman SD** (1997) Aluminum activates an anion channel in the apical cells of wheat roots. *Proc Natl Acad Sci USA* **94**: 6547–6552
- Sadowsky MJ, Schortemeyer M** (1997) Soil microbial responses to increased concentrations of atmospheric CO₂. *Global Change Biol* **3**: 217–224
- Skene KR, Kierans M, Sprent JI, Raven JA** (1996) Structural aspects of cluster root development and their possible significance for nutrient acquisition in *Grevillea robusta* (Proteaceae). *Ann Bot* **77**: 443–451
- Skene KR, Raven JA, Sprent JI** (1998a) Cluster root development in *Grevillea robusta* (Proteaceae). I. Xylem, pericycle, cortex, and epidermis development in a determinate root. *New Phytol* **138**: 725–732
- Skene KR, Sutherland JM, Raven JA, Sprent JI** (1998b) Cluster root development in *Grevillea robusta* (Proteaceae). II. The development of the endodermis in a determinate root and in an indeterminate, lateral root. *New Phytol* **138**: 733–742
- Stitt M** (1983) Citrate synthase. In HU Bergmeyer, ed, *Methods of Enzymatic Analysis*, Ed 3, Vol IV. Verlag Chemie, Weinheim, Germany, pp 353–358
- Thimann KV** (1936) Auxins and the growth of roots. *Am J Bot* **23**: 561–569
- Vance CP, Stade S, Maxwell CA** (1983) Alfalfa root nodule carbon dioxide fixation. I. Association with nitrogen fixation and incorporation of amino acids. *Plant Physiol* **72**: 469–473
- Varney GT, McCully ME** (1991) The branch roots of *Zea*. II. Developmental loss of the apical meristem in field-grown roots. *New Phytol* **118**: 535–546
- Vidal J, Chollet R** (1997) Regulatory phosphorylation of C₄ PEP carboxylase. *Trends Plant Sci* **2**: 230–237
- Whipps J** (1985) Effect of CO₂ concentrations on growth, carbon distribution and loss of carbon from the roots of maize. *J Exp Bot* **36**: 644–651
- Wightman F, Schneider EA, Thimann KV** (1980) Hormonal factors controlling the initiation and development of lateral roots. II. Effects of exogenous growth factors on lateral root formation in pea roots. *Physiol Plant* **49**: 304–314